Eur. Phys. J. C (2025) 85:1144
https://doi.org/10.1140/epjc/s10052-025-14890-8

THE EUROPEAN PHYSICAL JOURNAL C

Regular Article - Theoretical Physics

Weak gravity conjecture in ModMax black holes: weak cosmic censorship and photon sphere analysis

Saeed Noori Gashti[1,a], **Mohammad Ali S. Afshar**[1,2,b], **Mohammad Reza Alipour**[1,2,c], **İzzet Sakallı**[3,d], **Behnam Pourhassan**[1,4,5,e], **Jafar Sadeghi**[1,2,f]

[1] School of Physics, Damghan University, Damghan 3671645667, Iran
[2] Department of Physics, Faculty of Basic Sciences, University of Mazandaran, P. O. Box 47416-95447, Babolsar, Iran
[3] Physics Department, Eastern Mediterranean University, North Cyprus, via Mersin 10, 99628 Famagusta, Turkey
[4] Center for Theoretical Physics, Khazar University, 41 Mehseti Street, 1096 Baku, Azerbaijan
[5] Centre of Research Impact and Outcome, Chitkara University, Rajpura, Punjab 140401, India

Received: 23 April 2025 / Accepted: 3 October 2025

Abstract It seems that the regime of Hawking radiation and evaporation ultimately drives charged black holes toward super-extremality of the charge parameter and the dominance of extremal conditions. This progression, in turn, lays the groundwork for satisfying the necessary conditions for the Weak Gravity Conjecture (WGC). Preliminary studies indicate that black holes such as the Reissner–Nordström (RN) model, in their initial form, lack the capacity to sustain super-extremality of the charge parameter. If such conditions arise, these black holes transition into naked singularities – a scenario that is highly undesirable due to the loss of causality and the breakdown of space–time geometry. This raises whether the inability to sustain super-extremality is an inherent property of the model or a consequence of the approximations and precision limitations employed in its construction. To address this, we turned to the ModMax model, which represents an extension of the RN model. Our analysis revealed that the ModMax model not only accommodates super-extremality of the charge parameter but also, under certain conditions, emerges as a promising candidate for investigating the WGC. Furthermore, we independently observed how the inclusion of the de Sitter radius (ℓ) in the AdS model and $F(R)$ gravitational corrections – both of which enhance and complicate the model – can have a direct impact on the range of super-extremal charge tolerance which, in turn, provides the realization of the conditions necessary for the WGC.

Contents

1 Introduction . . . . . .
2 Photon sphere . . . . . .
3 Model I: ModMax BH . . . . . .
3.1 WGC with photon sphere monitoring . . . . . .
4 Model II: ModMax-AdS BH . . . . . .
4.1 WGC–WCCC connection . . . . . .
4.2 WGC with photon sphere monitoring . . . . . .
5 Model III: BH in $F(R)$-ModMax theory . . . . . .
5.1 WGC with photon sphere monitoring . . . . . .
6 Conclusion . . . . . .
References . . . . . .

1 Introduction

One of the most intriguing aspects in the study of charged black hole (BH) dynamics is the investigation of the conditions under which BHs achieve extremality and the phenomenon whereby the BH's charge parameter becomes super-extremal. In general, when examining BHs – and given the necessary conditions for their formation – researchers are always keen to ensure that gravity serves as the key determinant and primary justification for all the behaviors expected of a BH. However, since the concept of temperature and the gradual evaporation of BHs via Hawking radiation [1–3] was introduced, it has become evident that, for stan-

[a] e-mail: saeed.noorigashti@stu.umz.ac.ir (corresponding author)
[b] e-mail: m.a.s.afshar@gmail.com
[c] e-mail: mr.alipour@stu.umz.ac.ir
[d] e-mail: izzet.sakallı@emu.edu.tr
[e] e-mail: b.pourhassan@du.ac.ir
[f] e-mail: pouriya@ipm.ir

Published online: 13 October 2025

dard BHs, this evaporation regime eventually causes the BH to self-transition towards extremal and even super-extremal conditions [4–9]. As the BH approaches its extremal state – where Hawking temperature tends to zero, radiation ceases, the Cauchy and event horizons, if present, coincide, and most importantly, the charge-to-mass ratio increases beyond one – nothing remains stable or normal in this situation. Clearly, such conditions cannot persist as a stable phase for the rest of the BH's existence.

At these critical moments, either the concept of the BH must be abandoned as a studiable entity consistent with causality and general relativity (leading to a "Swampland" scenario for the survival of the gravitational model), or a shock is required. This necessary shock might be explained through the WGC, acting as a safeguard for causality and general relativity. Assuming the temporary dominance of electromagnetism over gravity, and using hypotheses such as Schwinger pair production, the conjecture proposes a way to separate excess charge from the BH, enabling its recovery and return to the realm of general relativity and causality. To provide a preliminary understanding of the concepts discussed in the article, a brief explanation of the WGC is given, though we strongly encourage interested readers to explore more detailed discussions in references such as [4–7]. A fundamental principle underlying the swampland program is the prohibition of global symmetries in quantum gravity, allowing only gauge symmetries as exceptions. In line with this principle, the WGC, which originates from this framework, serves as a benchmark for validating field theories in accordance with our empirical understanding. The WGC is founded on the premise that gravity must be the weakest force among all fundamental interactions [10]. The conjecture proposes a condition on effective field theories coupled to gravity (i.e., any consistent theory that arises from the combination of gravity and electromagnetism – or other gauge forces). It states that in any consistent quantum gravity theory, there must exist at least one particle with a charge-to-mass ratio greater than or equal to that of an extremal BH. In other words, there must exist at least one charged particle for which its electromagnetic repulsion is stronger than its gravitational attraction, thereby demonstrating gravity's relative weakness compared to electromagnetism for at least one particle.

The implications of this conjecture are significant: it prevents the existence of entirely and perpetually stable BHs under all conditions, which could otherwise lead to remnants that violate entropy bounds. Furthermore, the WGC ensures that BHs dominated by electromagnetism over gravity can decay, as charged particles satisfying the conjecture can be emitted [4–7]. For these conditions to be realized, a BH must inherently possess the capacity to manifest and sustain super-extremal charges ($q/m > 1$) within its initial structural configuration. However, preliminary studies indicate that some charged BHs – whether modeled via the simple linear electromagnetic framework of the Reissner–Nordström (RN) solution [8,9,11] or via more intricate non-linear formulations – are incapable of withstanding super-extremal charge conditions in their original form. When such conditions arise, the BH tends to evolve into a naked singularity – a scenario we strongly wish to avoid, given its implication of a breakdown in causality and space–time geometry. Therefore, among the various BH models, we must search for those that not only have the inherent capacity to develop super-extremal charges in their initial configuration but also preserve the fundamental conditions required of a BH; that is, they should not violate the Weak Cosmic Censorship Conjecture (WCCC) [11–18] and must continue to exhibit the general observational signatures of BHs, such as the presence of a photon sphere [8,9,19–21].

It is important to emphasize that one might question whether the mere non-violation of the WCCC and the presence of features like a photon sphere are sufficient for maintaining a BH's integrity. Note that we are not modeling new structures here. Instead, we are studying a model that, until a few steps prior, fully adhered to the general conditions of a BH. However, under the regime predicted for its evaporation, it is advancing, and even approaching, conditions of instability that could lead to its complete loss. Therefore, if, at the end of this evolutionary trajectory and proximity to instability, the model can still display simultaneous signs of life – such as non-violation of the WCCC or the presence of a photon sphere – there is reason for optimism that the condition holds. Subsequently, we extend our analysis by incorporating the de Sitter radius to assess whether introducing this parameter affects the model's ability to withstand super-extremal charges and facilitates the establishment of the initial conditions necessary for the realization of the WGC. In the final step, we will take a further step by considering gravitational $F(R)$ corrections applied to the four-dimensional ModMax model in order to investigate whether, with such modifications, our BH model can still, even if only temporarily, exhibit conditions in which electromagnetism supersedes gravity and thereby permit the occurrence of the WGC. In conclusion, by comparing these models, we aim to ascertain how each additional parameter incorporated into the BH action influences the capacity to sustain super-extremal charges.

2 Photon sphere

In this section, we delve into the photon sphere of BHs. To begin, we define key terms and utilize the relevant equations that characterize these BHs. Since we will deal with the static spherical model in this study, the general form of the line element is given by,

$$ds^2 = -f(r)dt^2 + \frac{dr^2}{g(r)} + h(r)\left(d\theta^2 + \sin^2\theta\, d\phi^2\right), \quad (1)$$

where $g(r) = f(r)$ and $h(r) = r^2$. Typically, to study null geodesics and achieve the photon sphere, an effective potential is required; due to the $\mathbb{Z}_2$ symmetry, it can be practically limited to the equatorial plane ($\theta = \pi/2$) without loss of generality. In general, after some calculation, it can be written in the following form [22,23],

$$\dot{r}^2 + V_{\text{eff}} = 0. \quad (2)$$

Here, the effective potential V_{eff} is expressed as,

$$V_{\text{eff}} = g(r)\left[\frac{L^2}{h(r)} - \frac{E^2}{f(r)}\right], \quad (3)$$

where E and L correspond to the photon's energy and angular momentum, associated with the Killing vector fields ∂_t and ∂_ϕ, respectively. Due to the spherical symmetry of the solution, the photon sphere occurs at a radial position r_{ps}, determined by the conditions:

$$V_{\text{eff}} = 0, \quad \partial_r V_{\text{eff}} = 0. \quad (4)$$

This leads to the equation

$$\left(\frac{f(r)}{h(r)}\right)'\Big|_{r=r_{\text{ps}}} = 0, \quad (5)$$

where the prime denotes differentiation with respect to r. For an unstable photon sphere, $\partial_{r,r} V_{\text{eff}}(r_{\text{ps}}) < 0$, while $\partial_{r,r} V_{\text{eff}}(r_{\text{ps}}) > 0$ corresponds to a stable photon sphere. Differentiating further yields,

$$f(r)h'(r) - f'(r)h(r) = 0. \quad (6)$$

At the BH horizon, where $f(r_h) = 0$, the first term vanishes, but the second term is typically nonzero. Hence, $r_{\text{ps}} \neq r_h$ in general. However, for an extremal BH – where the two horizons merge – we find $f(r_h) = 0$ and $f'(r_h) = 0$, making the photon sphere coincide with the extremal BH horizon.

In this article, instead of using the conventional method, we study the behavior of the photon sphere based on the topological method. In this method, the behavior of each photon sphere is analyzed by considering its topological charge. Since the methodology of this method has been well described and examined in various models in previous articles [22–27], we refrain from repeating the details and mention only the basic relationships. To explore the topology of the photon sphere, we introduce the regular potential function,

$$H(r,\theta) = \sqrt{-\frac{g_{tt}}{g_{\phi\phi}}} = \frac{1}{\sin\theta}\sqrt{\frac{f(r)}{h(r)}}. \quad (7)$$

The photon sphere radius is obtained as the root of $\partial_r H = 0$. Utilizing the vector field components $\phi = (\phi^r, \phi^\Theta)$, we define

$$\phi^r = \frac{\partial_r H}{\sqrt{g_{rr}}} = \sqrt{g(r)}\partial_r H, \quad \phi^\Theta = \frac{\partial_\theta H}{\sqrt{g_{\theta\theta}}} = \frac{\partial_\theta H}{\sqrt{h(r)}}. \quad (8)$$

The vector can be rewritten as,

$$\phi = \|\phi\| e^{i\Theta}, \quad \|\phi\| = \sqrt{\phi^a \phi_a}. \quad (9)$$

Thus, the vector field can alternatively be expressed as $\phi = \phi^r + i\phi^\Theta$, and the normalized vectors are given by,

$$n^a = \frac{\phi^a}{\|\phi\|}, \quad \text{with } (\phi^1 = \phi^r,\ \phi^2 = \phi^\Theta). \quad (10)$$

Given an effective potential H and an associated vector field ϕ, the locations of photon spheres are identified by the zeros of the radial component of ϕ. This vector field governs the orientation and topology of the surrounding field lines, allowing for an illustrative analogy: the behavior of field lines near an unstable photon sphere – corresponding to a local maximum of the potential – resembles that of lines encircling a negative electric charge. In contrast, stable photon spheres – associated with local minima – exhibit field line configurations analogous to those around a positive charge. This analogy, combined with the observed differences in the rotational behavior of the field lines, provides a natural framework for assigning a topological charge to each photon sphere. Previous investigations, including our own, have demonstrated that black holes with an event horizon typically possess an unstable photon sphere located outside the horizon. This configuration is characterized by a total topological charge of $PS = -1$, signifying the presence of at least one local maximum in the effective potential landscape [22–25]

3 Model I: ModMax BH

The spherically symmetric static (SSS) solution to the Einstein equations coupled with ModMax nonlinear electrodynamics (NLED), derived in [29], is characterized by three key parameters: the BH mass M, the BH charge Q, and the nonlinear parameter γ. The line element for this solution is expressed as [29,30],

$$ds^2 = g_{\mu\nu}dx^\mu dx^\nu = -f(r)dt^2 + \frac{dr^2}{f(r)} + r^2 d\Omega^2, \quad (11)$$

where the metric function $f(r)$ is given by,

$$f(r) = 1 - \frac{2M}{r} + \frac{e^{-\gamma}Q^2}{r^2}. \quad (12)$$

Here, the angular part of the metric is represented as,

$$d\Omega^2 = d\theta^2 + \sin^2\theta\, d\phi^2. \quad (13)$$

The charge Q can be purely electric ($Q = Q_e$), purely magnetic ($Q = Q_m$), or a combination of both (the dyonic case), such that

$$Q = \sqrt{Q_e^2 + Q_m^2}. \quad (14)$$

We assume the presence of a purely electric charge for all subsequent calculations. This metric describes a charged BH with horizons determined by the roots of the equation $f(r) = 0$. These roots are given by,

$$r_+ = r_h = M + \sqrt{M^2 - e^{-\gamma}Q^2},$$
$$r_- = M - \sqrt{M^2 - e^{-\gamma}Q^2}. \quad (15)$$

For the existence of an event horizon at r_h, the condition $0 \le e^{-\gamma}Q^2 \le M^2$ must be satisfied. The metric $g_{\mu\nu}$ in this form is regarded as the background metric for subsequent analyses. The metric function for the Reissner–Nordström BH (RN BH) is given as,

$$f_{\rm RN}(r) = 1 - \frac{2M}{r} + \frac{Q^2}{r^2}. \quad (16)$$

It is evident that the ModMax metric function $f(r)$ resembles the RN metric, but with a screened charge due to the presence of the exponential factor $e^{-\gamma}$. This screening effect allows the ModMax BH to accommodate a higher charge compared to the RN BH. Specifically: For the RN BH, the charge is constrained by $Q^2 \le M^2$. For the ModMax BH, the charge can satisfy the less restrictive condition $Q^2 \le e^{\gamma}M^2$. In order to compare the various black hole models and their associated parameter spaces,

The three-dimensional geometric visualizations presented in Fig. 1 provide crucial insights into the fundamental differences between classical and ModMax BH solutions, revealing how NLED systematically modifies spacetime curvature through a clear evolutionary pathway from the foundational Schwarzschild solution to the ModMax framework that enables super-extremal charge accommodation. The Schwarzschild baseline case (Fig. 1a) establishes the pure gravitational geometry with its characteristic $r_h = 2M$ horizon, serving as the reference point for all subsequent electromagnetic modifications, while the transition to the RN configuration (Fig. 1b) introduces linear Maxwell corrections where the Q^2/r^2 term competes with gravitational attraction, resulting in a reduced horizon radius of $r_h = 1.866M$ that reflects electromagnetic repulsion challenging gravitational dominance. The ModMax cases (Fig. 1c–f) reveal the transformative power of NLED through the exponential screening factor $e^{-\gamma}$, where systematic variation of γ demonstrates how this parameter acts as a "charge capacity regulator," enabling the BH to accommodate increasingly extreme charge-to-mass ratios while preserving horizon stability – with $\gamma = 1$ (Fig. 1c) comfortably satisfying the super-extremal condition $Q = M$ at $r_h = 1.308M$, $\gamma = 2$ (Fig. 1d) providing enhanced charge tolerance at $r_h = 1.930M$, and the intermediate case $\gamma = 0.5$ (Fig. 1e) bridging near-extremal RN behavior with full ModMax screening effects. Particularly noteworthy is the negative $\gamma = -0.3$ case (Fig. 1f), which produces $r_h = 1.993M$ approaching the Schwarzschild limit despite maintaining super-extremal charge $Q = M$, demonstrating that negative γ values enhance rather than screen electromagnetic effects through the amplification factor $e^{0.3} \approx 1.35$. From the WGC perspective, these visualizations illustrate why the ModMax framework succeeds where classical solutions fail: the ability to maintain stable horizons while accommodating super-extremal charges – clearly demonstrated by the preserved funnel geometries in cases (c) through (f) – provides the necessary foundation for WGC compatibility, while the smooth geometric transitions across parameter space suggest that the ModMax mechanism offers a robust pathway for resolving the tension between electromagnetic dominance and gravitational consistency that plagued earlier models.

We can also calculate the temperature of this model as follows,

$$T = \frac{1}{4\pi}\left(\frac{1}{r_h} - \frac{e^{-\gamma}Q^2}{r_h^3}\right). \quad (17)$$

When $T = 0$ we have,

$$r_h^{ext} = e^{-\frac{\gamma}{2}}Q. \quad (18)$$

Therefore, with respect to Eqs. (15) and (18) we have,

$$\frac{Q_{ext}}{M_{ext}} = e^{\frac{\gamma}{2}}. \quad (19)$$

According to the above relationship, for $\gamma > 0$, the WGC condition holds. So that for $\gamma \ll 1$, the relation in Eq. (19) can be expanded as follows,

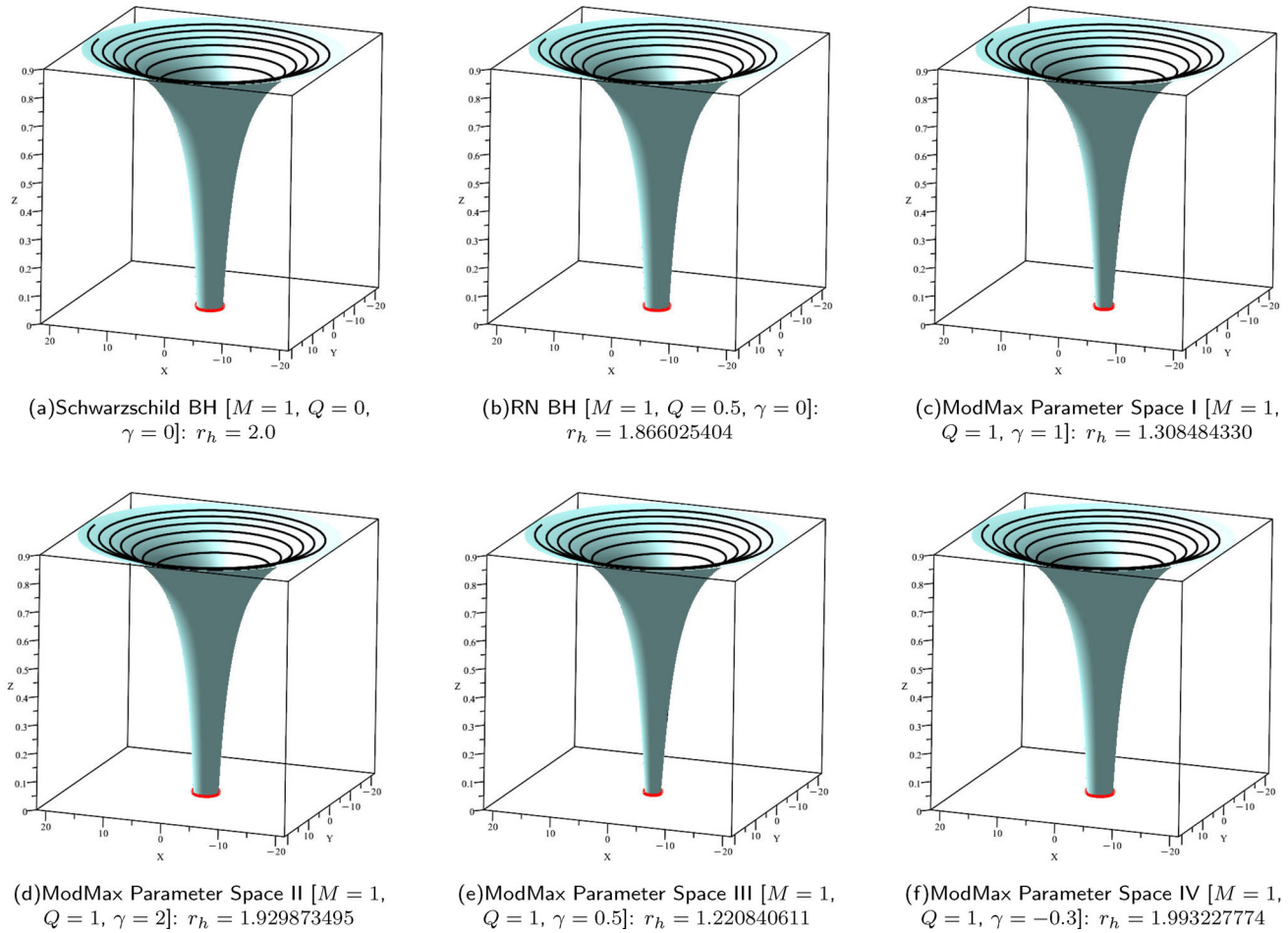

(a)Schwarzschild BH [$M = 1$, $Q = 0$, $\gamma = 0$]: $r_h = 2.0$

(b)RN BH [$M = 1$, $Q = 0.5$, $\gamma = 0$]: $r_h = 1.866025404$

(c)ModMax Parameter Space I [$M = 1$, $Q = 1$, $\gamma = 1$]: $r_h = 1.308484330$

(d)ModMax Parameter Space II [$M = 1$, $Q = 1$, $\gamma = 2$]: $r_h = 1.929873495$

(e)ModMax Parameter Space III [$M = 1$, $Q = 1$, $\gamma = 0.5$]: $r_h = 1.220840611$

(f)ModMax Parameter Space IV [$M = 1$, $Q = 1$, $\gamma = -0.3$]: $r_h = 1.993227774$

Fig. 1 Three-dimensional visualization of black hole geometries demonstrating the transition from classical solutions to ModMax nonlinear electrodynamics. **a** Schwarzschild BH ($\gamma = 0$, $Q = 0$) establishes the baseline uncharged geometry with event horizon at $r_h = 2M$. **b** Reissner–Nordström BH illustrates the standard linear Maxwell electrodynamics case, showing charge-induced modifications to the metric with a smaller horizon radius due to electromagnetic repulsion. **c–f** ModMax black hole configurations across different nonlinear parameter regimes reveal the systematic impact of the screening parameter γ on the geometric structure

$$\frac{Q_{ext}}{M_{ext}} = 1 + \frac{\gamma}{2} + \mathcal{O}(\gamma). \tag{20}$$

As evident from the equations and figures, Model I demonstrates structural changes with respect to the parameter γ. For all values of $\gamma > 0$, the WGC is satisfied for this structure, as clearly illustrated in Fig. 2. Furthermore, Fig. 3 reveals the presence of an unstable photon sphere ($PS = -1$) outside the event horizon, which serves as an initial indication of the preservation of the BH structure. Importantly, while maintaining the BH structure, the photon sphere offers intuitive support for the WGC. Simultaneously, compatibility between the two conjectures – the WGC and the WCCC – is achieved. Hence, this BH model demonstrates compatibility with the WGC.

3.1 WGC with photon sphere monitoring

According to Eqs. (7), (8) and (12), with $g(r) = f(r)$ and $h(r) = r^2$, we have,

$$\begin{aligned} \phi^r &= -\frac{e^{-\gamma}\csc(\theta)\left(2Q^2 - 3e^{\gamma/2}Qr + e^{\gamma}r^2\right)}{r^4}, \\ \phi^\theta &= -\frac{e^{-\frac{\gamma}{2}}\cot(\theta)\csc(\theta)\left(Q - e^{\gamma/2}r\right)}{r^3}. \end{aligned} \tag{21}$$

4 Model II: ModMax-AdS BH

The action governing Einstein's gravity, coupled with ModMax electrodynamics and a cosmological constant in a four-dimensional spacetime, can be expressed as [28],

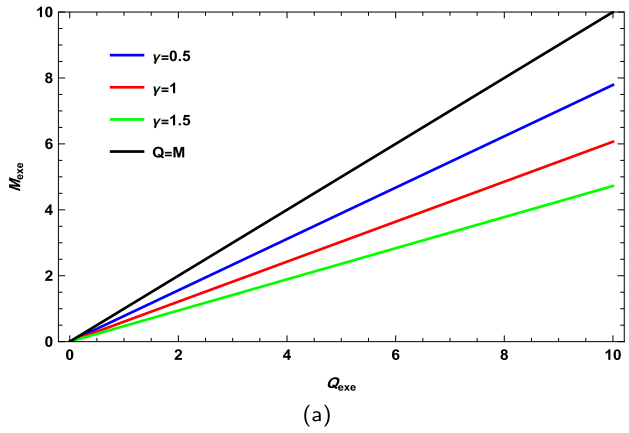

Fig. 2 The $(Q_{exe} - M_{exe})$ plane for different values of γ

$$\mathcal{I} = \frac{1}{16\pi}\int_{\partial\mathcal{M}} d^4x\sqrt{-g}\,[R - 2\Lambda - 4\mathcal{L}], \tag{22}$$

where R is the Ricci scalar, Λ is the cosmological constant, and $g = \det(g_{\mu\nu})$ represents the determinant of the metric tensor $g_{\mu\nu}$. For simplicity, the Newtonian gravitational constant G and the speed of light c are set to unity ($G = c = 1$). To include a radial electric field, we introduce the gauge potential,

$$A_\mu = y(r)\delta^t_\mu. \tag{23}$$

By utilizing the metric and the ModMax field equations,

$$\partial_\mu\left(\sqrt{-g}e^{-\gamma}F^{\mu\nu}\right) = 0, \tag{24}$$

we derive,

$$2y'(r) + ry''(r) = 0, \tag{25}$$

where the prime ($'$) and double prime ($''$) denote the first and second derivatives with respect to r, respectively. Solving this equation yields

$$y(r) = -\frac{Q}{r}, \tag{26}$$

where Q is an integration constant related to the electric charge. The electric field $E(r)$ can then be extracted using the electromagnetic field tensor, resulting in,

$$E(r) = \frac{Q}{r^2}e^{-\gamma}. \tag{27}$$

With further calculations from [28], the following differential equations are obtained,

$$\mathrm{Eq}_{tt} = \mathrm{Eq}_{rr} = rf'(r) + \Lambda r^2 - 1 + f(r) + \frac{Q^2}{r^2}e^{-\gamma} = 0, \tag{28}$$

and,

$$\mathrm{Eq}_{\theta\theta} = \mathrm{Eq}_{\phi\phi} = f''(r) + 2\Lambda + \frac{2}{r}f'(r) - \frac{2Q^2}{r^4}e^{-\gamma} = 0. \tag{29}$$

By solving these differential equations, the metric function $f(r)$ is found to be,

$$f(r) = 1 - \frac{2m_0}{r} - \frac{\Lambda r^2}{3} + \frac{Q^2e^{-\gamma}}{r^2}, \tag{30}$$

where m_0 is an integration constant representing the geometrical mass of the BH. Notably, this solution satisfies all components of the field equations simultaneously. When $\gamma = 0$, the metric reduces to the familiar RN (A)dS BH,

$$f(r) = 1 - \frac{2m_0}{r} - \frac{\Lambda r^2}{3} + \frac{Q^2}{r^2}. \tag{31}$$

Therefore, according to Eq. (30) and with respect to $\Lambda = -\frac{3}{l^2}$, the mass and temperature for this model are calculated in the following form,

$$M = \frac{e^{-\gamma}\left(l^2Q^2 + e^{\gamma}l^2r_h^2 + e^{\gamma}r_h^4\right)}{2l^2r_h}, \tag{32}$$

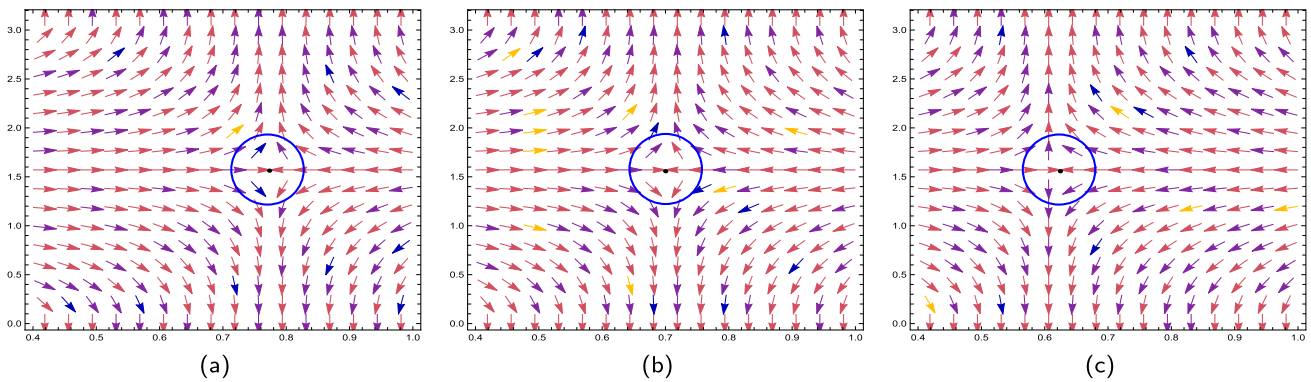

Fig. 3 The normal vector in the $(r - \theta)$ plane associated with the photon spheres. **a** $\gamma = 0.5$, $Q_{ext} = 0.5$, $M_{ext} = 0.3894$, $r_h^{ext} = 0.3894$. **b** $\gamma = 0.7$, $Q_{ext} = 0.5$, $M_{ext} = 0.35234$, $r_h^{ext} = 0.35234$. **c** $\gamma = 1$, $Q_{ext} = 0.5$, $M_{ext} = 0.30326$, $r_h^{ext} = 0.30326$

and,

$$T = \frac{1}{4\pi}\left(\frac{3r_h}{l^2} - \frac{e^{-\gamma}Q^2}{r_h^3} + \frac{1}{r_h}\right). \tag{33}$$

The WGC plays a central role within the swampland program, a framework that seeks to differentiate effective field theories (EFTs) that are compatible with quantum gravity (the "landscape") from those that are not (the "swampland"). As a guiding principle, the WGC ensures that gravity is always the weakest force in $U(1)$ gauge theories. This condition is satisfied by the existence of particles with a charge-to-mass ratio $q/m > 1$. The implications of the WGC are profound when applied to BH physics. Charged BHs are generally categorized based on the relationship between their charge Q and mass M as follows: (1) Subextremal BHs ($Q < M$): these are undercharged. (2) Extremal BHs ($Q = M$): these BHs lie at the threshold of being maximally charged. (3) Superextremal BHs ($Q > M$): these are overcharged. According to the WGC, extremal BHs should decay and throw superextremal particles, thereby preventing the formation of naked singularities and maintaining consistency with the WCCC. If the WGC is violated, BHs could transition into superextremal states, exposing singularities that conflict with the WCCC and established physical laws. Consequently, the existence of superextremal particles is critical for ensuring both the stability and consistent evaporation of BHs, emphasizing their role in preserving the delicate interplay of forces described by the WGC.

Thermodynamics provides an essential framework for understanding BH behavior, offering insights into stability, decay mechanisms, and alignment with the WGC. Researchers utilize this framework to test the conjecture by examining cosmic phenomena, BH classifications, and theoretical predictions for observable evidence. This systematic approach not only supports the WGC's foundation but also strengthens the connection between quantum mechanics and cosmology, contributing to a more comprehensive understanding of fundamental principles.

To further explore the WGC and the WCCC, we study the metric of ModMax BHs in AdS spacetimes, focusing on their horizon structure and physical properties. The event horizon radius is determined by solving the condition $f(r) = 0$, where M and Q denote the BH's mass and charge, respectively. In RN BHs, when $Q > M$, the BH lacks an event horizon, leaving its singularity exposed to external observers as a naked singularity. This scenario directly contradicts the WCCC, which posits that singularities must always be hidden by event horizons. By simultaneously solving the metric equation and the extremality condition (derived by setting its derivative or temperature to zero), we establish the conditions under which the WGC and the WCCC are satisfied. Since the WGC and WCCC are not universally valid for all BHs, our investigation focuses on a specific scenario where these conjectures cannot simultaneously hold without the inclusion of the ModMax parameter. By isolating ModMax parameter-dependent terms in the metric, we identify configurations where the WCCC is satisfied alongside the WGC, at least in extremal cases. Using well-established relationships for the WGC, we calculate the extremal limit and determine the range of parameters where the WGC holds true.

Numerical methods are then employed to explore the regions of compatibility between the WGC and the WCCC, given the impracticality of obtaining an analytical solution for the higher-order terms in the equations. If a region exists where both conjectures are satisfied at critical or extremal points, this compatibility range can potentially extend to other areas of the BH parameter space. By examining various BH classes and categorizing them based on their properties, we identify suitable candidates for probing quantum gravity concepts. These classifications provide a foundation for extensive research, enabling a deeper understanding of BH physics while upholding essential physical principles. Through this rigorous approach, we contribute to the broader objectives of the swampland program, reinforcing its role in bridging quantum mechanics, cosmology, and fundamental physics. For further study, you can see [31–84]. To determine the extremality limit, we calculate the quantities r_h^{ext} and M_{ext} with respect to Eqs. (30), (32) and (33). Thus, we have,

$$r_h^{ext} = \frac{\sqrt{e^{-\frac{\gamma}{2}} l\sqrt{e^{\gamma}l^2 + 12Q^2} - l^2}}{\sqrt{6}}. \tag{34}$$

Using r_h^{ext} in the mass equation to determine the extremality limit, we can establish the inequality $(q^2/m^2) \geq (Q^2/M^2)_{ext}$,

$$M_{ext} = \frac{e^{-\gamma}\left(-e^{\gamma}l^2 + e^{\gamma/2}l\sqrt{e^{\gamma}l^2 + 12Q^2} + 12Q^2\right)}{3\sqrt{6}\sqrt{l\left(e^{-\frac{\gamma}{2}}\sqrt{e^{\gamma}l^2 + 12Q^2} - l\right)}}. \tag{35}$$

We believe it is important to clarify the motivation behind our focus on the extremal mass, particularly in the context of black hole evaporation and the Weak Gravity Conjecture (WGC). According to the standard framework of black hole evaporation, especially for charged black holes, the mass typically exceeds the charge. As the black hole radiates, this imbalance drives the system toward an extremal configuration – characterized by vanishing temperature and the cessation of Hawking radiation, rendering the black hole thermodynamically inert. However, such extremal states are known to be unstable, and the black hole must eventually transition

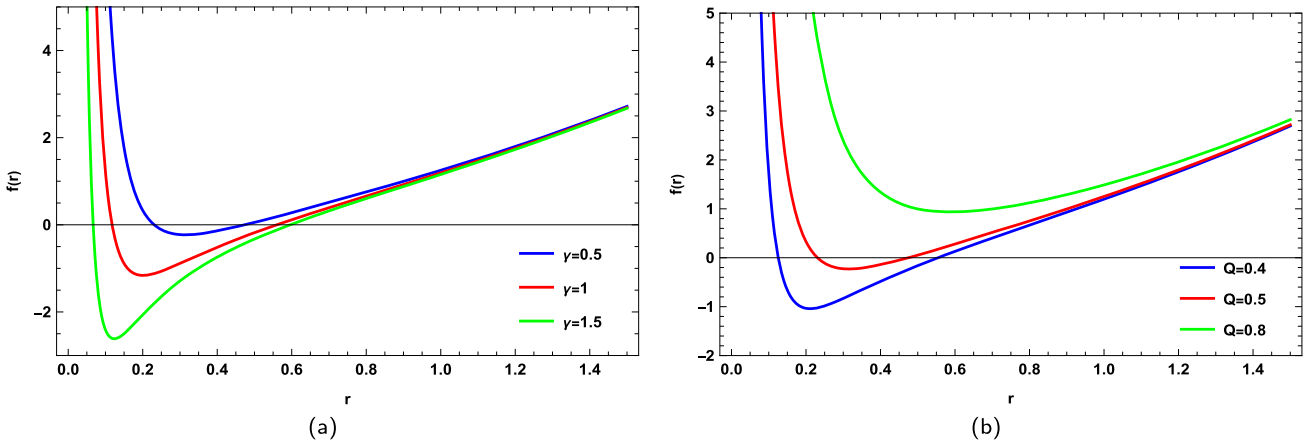

Fig. 4 The metric function with $l = 1$ and $M = 0.45$. **a** $Q = 0.5$ and various γ, **b** $\gamma = 0.5$ and various Q

away from this regime. In the thermodynamic evaporation process, the system can emit particles with super-extremal charge-to-mass ratios (i.e., particles for which $q/m > 1$ or $\frac{q^2}{m^2} \geq \left(\frac{Q^2}{M^2}\right)_{\text{ext}}$ holds, with q and m denoting the charge and mass of the test particle, and Q and M representing the charge and mass of the black hole, respectively). The emission of such particles allows the black hole to shed excess charge and return to a non-extremal, physically viable state. This mechanism is precisely what the WGC anticipates: that gravity should be the weakest force, and hence there must exist particles with charge-to-mass ratios exceeding that of extremal black holes. Therefore, computing the extremal mass is of central importance, as it marks the threshold at which the black hole approaches the WGC limit. This calculation not only informs the thermodynamic endpoint of evaporation but also provides insight into the consistency of the theory with quantum gravity expectations.

4.1 WGC–WCCC connection

Figure 4 presents the metric functions for varying free parameters, including different values of γ and the electric charge. This visualization forms the basis for analyzing the compatibility between the WGC and the WCCC in the forthcoming calculations.

For Model II, structural changes influenced by the cosmological constant and the parameter γ yield slightly different results. In this case, the WGC does not hold across all intervals, and compatibility is limited to specific ranges. At these points, the WCCC must also hold for the BH to have an event horizon.

As demonstrated in Fig. 5, larger values of γ correspond to a broader range of compatibility with the WGC – a result that adds significant appeal to this model.

Specifically, the parameter γ exhibits a direct relationship with the WGC, as shown in Figs. 6 and 7 for various parameter values. Within these ranges, an unstable photon sphere ($PS = -1$) is also observed. Additionally, the WCCC remains valid at these points, where the photon sphere provides further intuitive support for the structure as well as for the WGC.

Moreover, the compatibility of both conjectures is simultaneously preserved. Another parameter of particular importance is the anti-de Sitter (AdS) radius, which increases as the compatibility range for the WGC expands, as illustrated in Fig. 5.

4.2 WGC with photon sphere monitoring

According to Eqs. (7), (8) and (30), with $g(r) = f(r)$ and $h(r) = r^2$, we have,

$$\begin{aligned} \phi^r &= -\frac{\csc(\theta)\left(r(r-3M)+2e^{-\gamma}Q^2\right)}{r^4}, \\ \phi^\theta &= -\frac{\cot(\theta)\csc(\theta)\sqrt{\frac{r^2}{l^2}-\frac{2M}{r}+\frac{e^{-\gamma}Q^2}{r^2}+1}}{r^2}. \end{aligned} \tag{36}$$

5 Model III: BH in $F(R)$-ModMax theory

Here, we continue our calculations with the BH solutions in $F(R)$-ModMax theory [85]. We begin by considering a static, spherically symmetric spacetime described by the line element,

$$ds^2 = -g(r)\,dt^2 + \frac{dr^2}{g(r)} + r^2\left(d\theta^2 + \sin^2\theta\, d\phi^2\right), \tag{37}$$

We define $F(R) = R + f(R)$, where R denotes the scalar curvature and $f(R)$ represents a function dependent on R. Throughout this paper, we adopt natural units by setting the Newtonian gravitational constant and the speed of light to

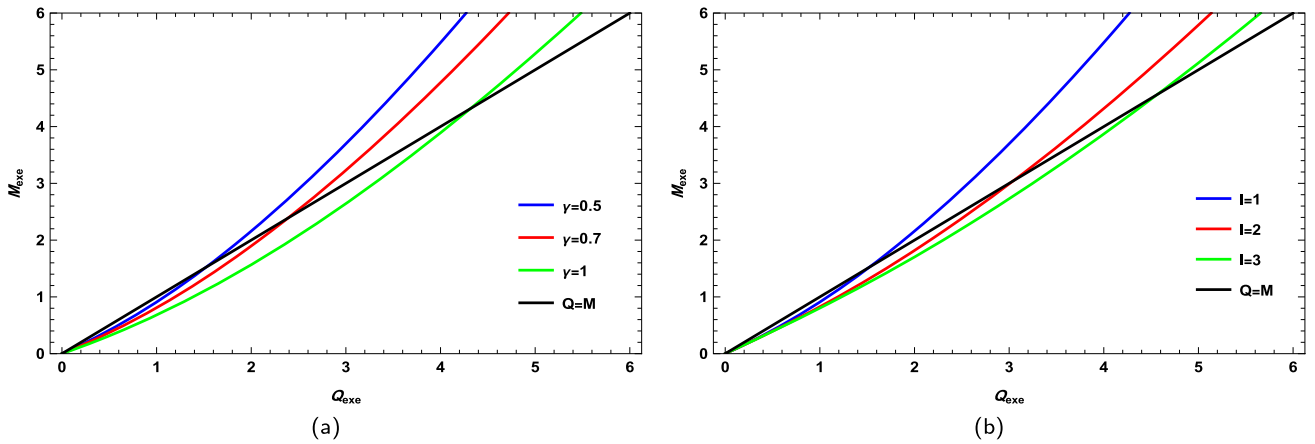

Fig. 5 The $(Q_{exe} - M_{exe})$ plane for **a** different values of γ with $l = 1$, and **b** different values of l with $\gamma = 0.5$

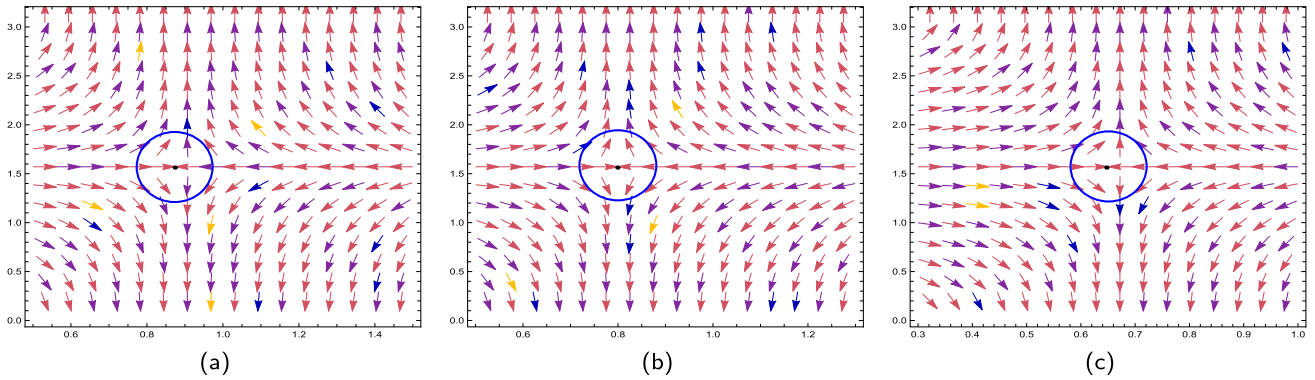

Fig. 6 The normal vector in the $(r - \theta)$ plane associated with the photon spheres. **a** $\gamma = 0.5$, $Q_{ext} = 0.5$, $M_{ext} = 0.412609$, $r_h^{ext} = 0.33644$. **b** $\gamma = 0.7$, $Q_{ext} = 0.5$, $M_{ext} = 0.3701312$, $r_h^{ext} = 0.31035$. **c** $\gamma = 1$, $Q_{ext} = 0.5$, $M_{ext} = 0.31511$, $r_h^{ext} = 0.27398$ with respect to $l = 1$

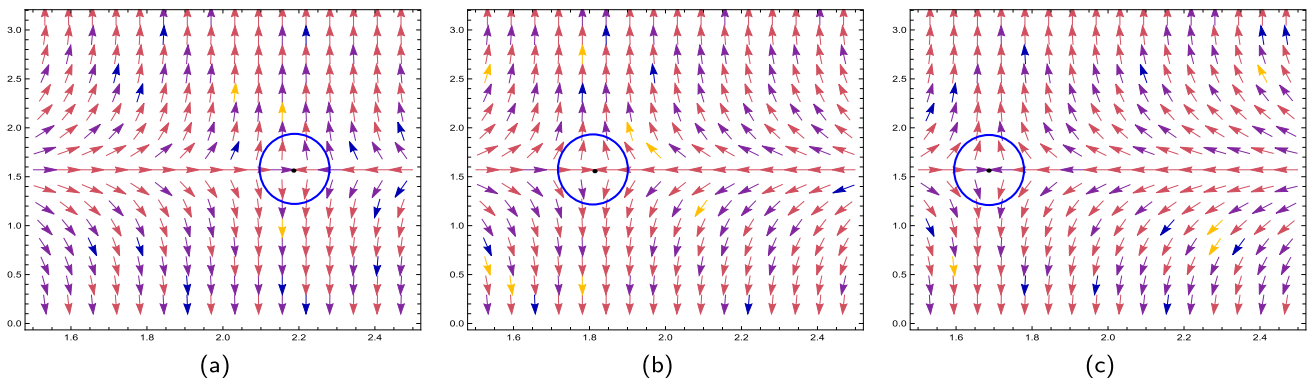

Fig. 7 The normal vector in the $(r - \theta)$ plane associated with the photon spheres. **a** $l = 1$, $Q_{ext} = 1$, $M_{ext} = 0.90935$, $r_h^{ext} = 0.559347$. **b** $l = 2$, $Q_{ext} = 1$, $M_{ext} = 0.82522$, $r_h^{ext} = 0.672886$. **c** $l = 3$, $Q_{ext} = 1$, $M_{ext} = 0.80193$, $r_h^{ext} = 0.719252$ with respect to $\gamma = 0.5$.

unity, i.e., $G = c = 1$. In general, the equations governing $F(R)$ gravity coupled with a nonlinear matter field (such as the ModMax field) are highly complex. As a result, obtaining an exact analytical solution can pose significant challenges. To address this, one can consider a traceless energy-momentum tensor for the nonlinear matter field. This approach allows for the derivation of an exact solution in $F(R)$ gravity coupled to the ModMax field. For a BH solution with constant scalar curvature, the trace of the stress-energy tensor $T_{\mu\nu}$ must vanish [86,87]. By assuming the scalar curvature R is constant, $R = R_0 =$ constant, the trace of the field equations,

$$R_{\mu\nu}(1 + f_R) - g_{\mu\nu}\frac{F(R)}{2} + g_{\mu\nu}\nabla^2 f_R - \nabla_\mu\nabla_\nu f_R = 8\pi T_{\mu\nu},$$

simplifies to,

$$R_0\,(1+f_{R_0})-2\,(R_0+f(R_0))=0, \tag{38}$$

where $f_{R_0}\equiv \frac{df}{dR}\Big|_{R=R_0}$. Solving this equation yields,

$$R_0=\frac{2f(R_0)}{f_{R_0}-1}. \tag{39}$$

By substituting Eq. (39) into the field equations, the equations of motion in $F(R)$-ModMax theory can be expressed as,

$$R_{\mu\nu}\,(1+f_{R_0})-\frac{g_{\mu\nu}}{4}R_0\,(1+f_{R_0})=8\pi T_{\mu\nu}. \tag{40}$$

It is worth noting that these equations reduce to the equations for general relativity (GR) coupled to the ModMax field when $f_{R_0}=0$. By employing the above differential equations and assuming $R=R_0=$ constant, one can derive an exact solution. After thorough calculations, the metric function takes the form,

$$g(r)=1-\frac{m_0}{r}-\frac{R_0r^2}{12}+\frac{Q^2e^{-\gamma}}{(1+f_{R_0})\,r^2}, \tag{41}$$

where m_0 is an integration constant associated with the geometric mass of the BH. Importantly, the derived solution satisfies the field equations (Eq. (40)) under the constraint $f_{R_0}\neq -1$, ensuring physical solutions. The effects of ModMax theory are evident in the fourth term of Eq. (41), while the contributions of $F(R)$ gravity manifest in both the third and fourth terms. Notably, when $f_{R_0}=0$, $R_0=4\Lambda$, and $\gamma=0$, the solution reduces to the RN-(A)dS BH, with the metric function given by,

$$g(r)=1-\frac{m_0}{r}-\frac{\Lambda r^2}{3}+\frac{Q^2}{r^2}. \tag{42}$$

We analyze the conserved and thermodynamic quantities of electrically charged BHs within the framework of $F(R)$-ModMax theory. The starting point involves determining the Hawking temperature of these BHs. The Hawking temperature is computed as,

$$T=\frac{\kappa}{2\pi}, \tag{43}$$

where κ represents the surface gravity of the BH, given by,

$$\kappa=\left((-\frac{1}{2})\nabla_\mu\chi_\nu\,\nabla^\mu\chi^\nu\right)^{1/2}=\frac{g'_{tt}}{2\sqrt{-g_{tt}g_{rr}}}\Big|_{r=r_h}=\frac{g'(r)}{2}\Big|_{r=r_h}, \tag{44}$$

where r_h is the radius of the event horizon, and $\chi=\partial_t$ is the Killing vector associated with the BH spacetime. Before obtaining the Hawking temperature, it is essential to derive an expression for the BH mass m_0 in terms of the event horizon radius r_h, the curvature parameter R_0, and the electric charge q. Solving the equation $g(r)=0$ yields,

$$m_0=r_h-\frac{R_0r_h^3}{12}+\frac{Q^2e^{-\gamma}}{(1+f_{R_0})r_h}, \tag{45}$$

where m_0 represents an integration constant related to the geometric mass of the BH. Using the metric function derived in Eq. (41) and substituting m_0 from Eq. (45) into the expression for surface gravity (Eq. (44)), the surface gravity becomes,

$$\kappa=\frac{1}{2r_h}-\frac{R_0r_h}{8}-\frac{Q^2e^{-\gamma}}{2(1+f_{R_0})r_h^3}. \tag{46}$$

Subsequently, the Hawking temperature is obtained by substituting Eq. (46) into Eq. (43), leading to,

$$T=\frac{1}{4\pi r_h}-\frac{R_0r_h}{16\pi}-\frac{Q^2e^{-\gamma}}{4\pi(1+f_{R_0})r_h^3}. \tag{47}$$

As shown, the Hawking temperature of BHs in $F(R)$-ModMax theory depends on various parameters, including the electric charge Q, the curvature parameters of $F(R)$ gravity (f_{R_0} and R_0), and the ModMax parameter γ. The mass of the BH is calculated as

$$M=\frac{e^{-\gamma}\,Q^2}{2f_{R_0}r_h+2r_h}-\frac{r_h^3R_0}{24}+\frac{r_h}{2}, \tag{48}$$

and with $T=0$, the extremal radius r_h^{ext} is calculated as follows,

$$r_h^{ext}=\sqrt{2}\sqrt{-\frac{\sqrt{e^\gamma\,(f_{R_0}+1)\left(e^\gamma+e^\gamma f_{R_0}+Q^2(-R_0)\right)}}{e^\gamma f_{R_0}R_0+e^\gamma R_0}+\frac{e^\gamma f_{R_0}}{e^\gamma f_{R_0}R_0+e^\gamma R_0}+\frac{e^\gamma}{e^\gamma f_{R_0}R_0+e^\gamma R_0}}. \tag{49}$$

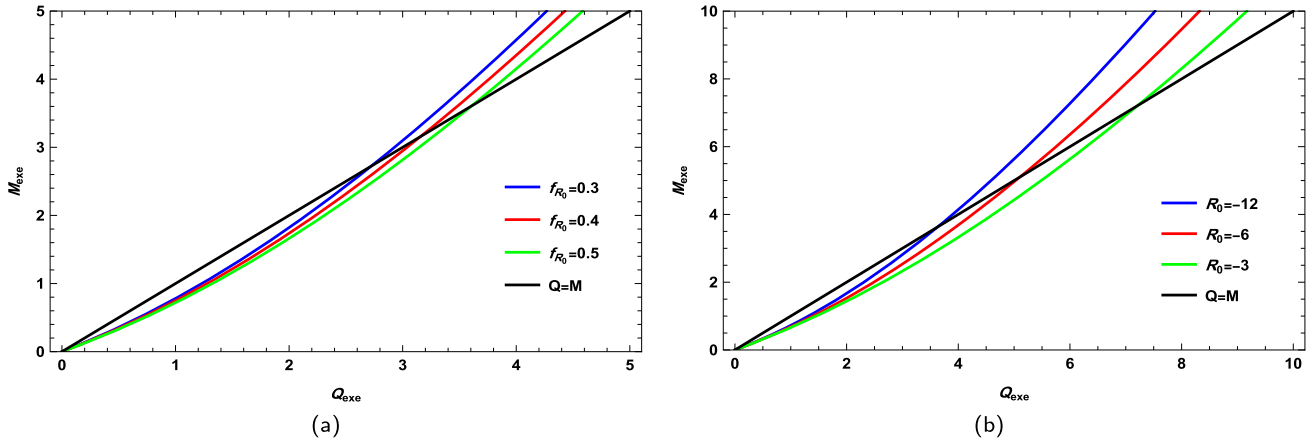

Fig. 8 The $(Q_{exe} - M_{exe})$ plane for **a** different values of f_{R_0} with $R_0 = -12$ and $\gamma = 0.5$, and **b** different values of R_0 with $f_{R_0} = 0.5$ and $\gamma = 0.5$

So, we have,

$$M_{ext}=\frac{\left(\sqrt{2}e^{-\gamma}Q\right)\left(2e^{\gamma}(f_{R_0}+1)+\sqrt{e^{\gamma}(f_{R_0}+1)\left(e^{\gamma}(f_{R_0}+1)-Q^2R_0\right)}\right)}{3(f_{R_0}+1)\sqrt{e^{\gamma}(f_{R_0}+1)+\sqrt{e^{\gamma}(f_{R_0}+1)\left(e^{\gamma}(f_{R_0}+1)-Q^2R_0\right)}}}. \tag{50}$$

5.1 WGC with photon sphere monitoring

According to Eqs. (7), (8) and (41), with $g(r) = f(r)$ and $h(r) = r^2$, we have,

$$\begin{aligned}\phi^r &= \frac{\csc(\theta)\left(r(r-3M)+\frac{2e^{-\gamma}Q^2}{1+f_{R_0}}\right)}{r^4},\\ \phi^\theta &= -\frac{\cot(\theta)\csc(\theta)\sqrt{\frac{e^{-\gamma}Q^2}{(1+f_{R_0})r^2}-\frac{2M}{r}-\frac{r^2R_0}{12}+1}}{r^2}.\end{aligned} \tag{51}$$

In Model III, additional noteworthy points emerge that distinguish it from the previous two models. For values of $R_0 > 0$, the structure reflects a de Sitter configuration, whereas for $R_0 < 0$, it adopts an anti-de Sitter (AdS) configuration. This study focuses on the AdS configuration, assuming $R_0 < 0$. In this model, the gravitational corrections play a crucial role; a larger range of the correction parameter corresponds to a higher probability of satisfying the WGC, as shown in Fig. 8. Since the parameter R_0 is inversely related to the AdS radius, a reduction in R_0 enhances the compatibility range for the WGC. Additionally, Fig. 9 confirms the presence of an unstable photon sphere ($PS = -1$) for the specified parameters. This provides strong intuitive support for the WGC and highlights its compatibility with the WCCC, as reflected in the diagrams.

To facilitate a comparative analysis of the three models with respect to the WGC, Fig. 10 offers a clear depiction of the compatibility range for each model under different parameter values. Notably, Model I exhibits compatibility with the WGC for any value of γ, whereas Models II and III are subject to stricter constraints. As detailed in the text, a classification based on the degree of compatibility with the WGC can be established, ranking the models in ascending order: Model II, Model III, and Model I. This classification indicates that Model I achieves the highest level of compatibility, while Model II demonstrates the lowest.

6 Conclusion

This study effectively investigates the critical challenge of reconciling the WGC and the WCCC within the ModMax BH framework. Through a meticulous examination of the parameter space, we identify specific conditions under which these two seemingly opposing principles achieve coherence. To substantiate this alignment, we further explore photon spheres from a topological perspective, providing valuable insights into their role in this compatibility. The topological approach, which has garnered significant attention in the scientific community, not only advances our understanding of photon spheres but also explores phase transitions in BH thermodynamics. This growing body of research underscores the importance of topology in bridging theoretical and thermodynamic aspects of BHs. For further study, you can see [24,25,88–121].

As stated earlier, our motivation for studying this topic was to investigate why a basic and fundamental model such as RN BHs, when the charge parameter becomes superextremal, loses its ability to exist in the extremal form and instead transforms into a naked singularity. This phenomenon, to

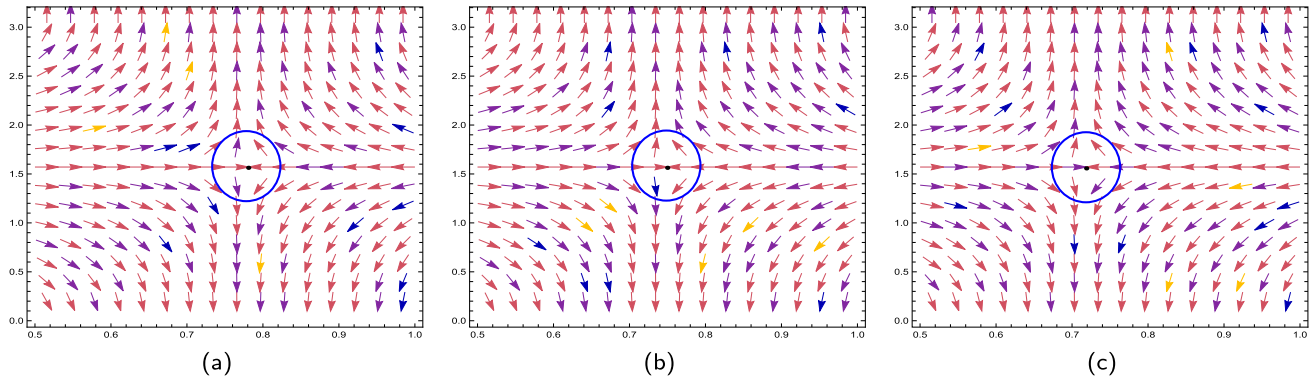

Fig. 9 The normal vector in the $(r-\theta)$ plane associated with the photon spheres. **a** $f_{R_0}=0.3$, $Q_{ext}=0.5$, $M_{ext}=0.35788$, $r_h^{ext}=0.30251$. **b** $f_{R_0}=0.4$, $Q_{ext}=0.5$, $M_{ext}=0.34390$, $r_h^{ext}=0.29339$. **c** $f_{R_0}=0.5$, $Q_{ext}=0.5$, $M_{ext}=0.33142$, $r_h^{ext}=0.28508$ with respect to $\gamma=0.5$ and $R_0=-12$

some extent, conflicts with the WGC, raising the question of whether this conflict stems from intrinsic properties of the Maxwell field or the degree of precision employed in formulating its electromagnetic component.

To address this, we considered the ModMax model, which represents a more accurate extension of Maxwellian conditions. The exponential function introduced in the ModMax model reduces to the RN model when only the first term (the least precise approximation) is retained. Our analysis demonstrates that incorporating higher-order terms of the charge in the extremal BH leads to the WGC condition being satisfied for all mass values when γ is positive. Furthermore, this condition strengthens as γ increases. This observation supports the hypothesis that electromagnetic models failing to exhibit conditions conducive to the emergence of the WGC may require corrections involving higher-order charge terms. In other words, this conjecture appears to possess theoretical comprehensiveness at a foundational level. However, additional observations and practical experiments are necessary for further verification. Subsequently, we examined the AdS model, which also revealed the intolerance of the RN model in this space and its inability to maintain a BH structure under superextremal charge conditions.

Under these circumstances, the ModMax BH satisfies the WGC condition in the extremal state but with certain restrictions. Specifically, the condition does not hold for all BH masses. Instead, for BHs with lower masses, the WGC condition persists, and with increasing γ and AdS radius, the range of validity for the WGC expands. This extension enables heavier BHs to satisfy the conjecture. Additionally, curvature corrections, often framed as $F(R)$ gravity, have been proposed to address theoretical weaknesses in BH models – such as naked singularities and the accelerated expansion of the universe – without invoking dark energy. By replacing curvature with a generalized function, $F(R)$ gravity offers solutions involving higher-order field equations. Our study aimed

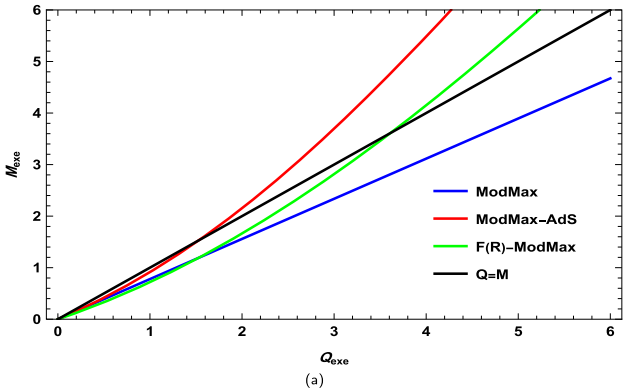

Fig. 10 The $(Q_{exe}-M_{exe})$ plane for different ModMax BHs with $R_0=-\frac{12}{l^2}$, $l=1$, $R_0=-12$, $f_{R_0}=0.5$ and $\gamma=0.5$

to evaluate whether the WGC remains applicable under this correction, specifically within the corrected ModMax model.

Our findings suggest that the WGC condition can indeed be satisfied for certain mass ranges of this BH, with the validity range increasing as $F(R)$ corrections intensify, accommodating BHs with greater rigidity. Finally, we compared the results for these three BH models in the extremal state, as illustrated in Fig. 10. Based on these observations, all three studied models demonstrate initial conditions qualifying them as candidates for WGC validation.

The pure ModMax model stands out by encompassing a broader range of BH masses, including both lighter and heavier BHs. Conversely, the gravitational correction $F(R)$ and the AdS models introduce constraints that limit the conjecture's applicability to lighter BHs. However, greater corrections and higher γ values extend the conditions to include heavier BHs. Despite the theoretical differences between the AdS and corrected models, a comparison can be drawn by considering the condition $(R_0=-\frac{12}{l^2})$. As shown in Fig. 10, gravitational corrections offer more compatible conditions for WGC validation.

Acknowledgements We sincerely thank the editor and referee for their constructive comments and valuable suggestions that have significantly improved the quality and clarity of our manuscript. The work of Saeed Noori Gashti is supported by the Iran National Science Foundation (INSF). This work is based upon research funded by the INSF under project No.4038260. İ. S thanks EMU, TÜBİTAK, ANKOS, and SCOAP3 for academic and/or financial support. He also acknowledges the networking support from COST Actions CA22113, CA21106, CA23130, CA21136, and CA23115.

Data Availability Statement This manuscript has no associated data. [Author's comment: Data sharing not applicable to this article as no datasets were generated or analysed during the current study.]

Code Availability Statement This manuscript has no associated code/software. [Author's comment: Code/Software sharing not applicable to this article as no code/software was generated or analysed during the current study.]

Funded by SCOAP[3].

References

1. S.W. Hawking, Black hole explosions? Nature **248**(5443), 30–1 (1974)
2. D.N. Page, Hawking radiation and black hole thermodynamics. New J. Phys. **7**(1), 203 (2005)
3. D.N. Page, Particle emission rates from a black hole. II. Massless particles from a rotating hole. Phys. Rev. D **14**(12), 3260 (1976)
4. T. Rudelius, An introduction to the weak gravity conjecture. Contemp. Phys. **64**(4), 282–95 (2023)
5. D. Harlow, B. Heidenreich, M. Reece, T. Rudelius, Weak gravity conjecture. Rev. Mod. Phys. **95**(3), 035003 (2023)
6. C. Cheung, G.N. Remmen, Naturalness and the weak gravity conjecture. Phys. Rev. Lett. **113**(5), 051601 (2014)
7. E. Palti, The weak gravity conjecture and scalar fields. J. High Energy Phys. **2017**(8), 1–26 (2017)
8. M.A. Afshar, J. Sadeghi, Mutual influence of photon sphere and non-commutative parameter in various non-commutative black holes: Towards evidence for WGC. Phys. Dark Universe **1**(47), 101814 (2025)
9. M.A. Afshar, J. Sadeghi, WGC as WCCC protector: the synergistic effects of various parameters in non-commutative black holes for identifying WGC candidate models. Nucl. Phys. B **1014**, 116872 (2025). arXiv:2412.00079
10. N. Arkani-Hamed, L. Motl, A. Nicolis, C. Vafa, The String landscape, black holes and gravity as the weakest force. J. High Energy Phys. **2007**(06), 060 (2007)
11. M.R. Alipour, J. Sadeghi, M. Shokri, WGC and WCC for charged black holes with quintessence and cloud of strings. Eur. Phys. J. C **83**(7), 640 (2023)
12. J. Sadeghi, S.N. Gashti, Influences of perfect fluid dark matter on coinciding validity of the weak gravity and weak cosmic censorship conjectures for Kerr-Newman black hole. Nucl. Phys. B **1**(1006), 116657 (2024)
13. J. Sadeghi, S.N. Gashti, Reissner–Nordström black holes surrounded by perfect fluid dark matter: testing the viability of weak gravity conjecture and weak cosmic censorship conjecture simultaneously. Phys. Lett. B **1**(853), 138651 (2024)
14. A. Anand, S.N. Gashti, M.R. Alipour, M.A. Afshar, Analyzing WGC and WCCC through charged scalar fields fluxes with charged AdS black holes surrounded by perfect fluid dark matter in the CFT thermodynamics. Nucl. Phys. B **1**(1013), 116857 (2025)
15. M.R. Alipour, J. Sadeghi, M. Shokri, WGC and WCCC of black holes with quintessence and cloud strings in RPS space. Nucl. Phys. B (2023)
16. J. Sadeghi, S.N. Gashti, M.R. Alipour, M.A. Afshar, Weak cosmic censorship and weak gravity conjectures in CFT thermodynamics. J. High Energy Astrophys. **1**(44), 482–493 (2024)
17. R. Ghosh, C. Fairoos, S. Sarkar, Overcharging higher curvature black holes. Phys. Rev. D **100**(12), 124019 (2019)
18. R. Ghosh, A.K. Mishra, S. Sarkar, Overcharging extremal black holes. Phys. Rev. D **104**(10), 104043 (2021)
19. M.R. Alipour, M.A.S. Afshar, S. Noori Gashti, J. Sadeghi, Weak gravity conjecture validation with photon spheres of quantum corrected Reissner–Nordstrom–AdS black holes in Kiselev spacetime. Eur. Phys. J. C **85**(2), 138 (2025)
20. M.R. Alipour, S.N. Gashti, B. Pourhassan, I. Sakallı, Reconciling the weak gravity and weak cosmic censorship conjectures in Einstein–Euler–Heisenberg-AdS black holes. arXiv preprint arXiv:2504.03453 (2025)
21. S.N. Gashti, I. Sakallı, B. Pourhassan, Thermodynamic topology, photon spheres, and evidence for weak gravity conjecture in charged black holes with perfect fluid within Rastall theory. arXiv preprint arXiv:2410.14492 (2024)
22. P.V.P. Cunha, E. Berti, C.A.R. Herdeiro, Light-ring stability for ultracompact objects. Phys. Rev. Lett. **119**(25), 251102 (2017)
23. S.-W. Wei, Topological charge and black hole photon spheres. Phys. Rev. D **102**(6), 064039 (2020)
24. J. Sadeghi, M.A.S. Afshar, The role of topological photon spheres in constraining the parameters of black holes. Astropart. Phys. **162**, 102994 (2024)
25. M.A.S. Afshar, J. Sadeghi, Effective potential and topological photon spheres: a novel approach to black hole parameter classification. Chin. Phys. C **49**, 035107 (2024)
26. J. Sadeghi, M.A. Afshar, S.N. Gashti, M.R. Alipour, Thermodynamic topology and photon spheres in the hyperscaling violating black holes. Astropart. Phys. **1**(156), 102920 (2024)
27. M.A. Afshar, J. Sadeghi, Mechanisms behind the Aschenbach effect in non-rotating black hole spacetime. Ann. Phys. **11**, 169953 (2025)
28. B.E. Panah, N. Heidari, Some aspects of ModMax (A) dS black holes: thermodynamics properties, heat engine, shadow, null geodesic and light trajectory. J. High Energy Astrophys. **45**, 181–193 (2025)
29. D. Flores-Alfonso et al., Black holes and gravitational waves sourced by non-linear duality rotation-invariant conformal electromagnetic matter. Phys. Lett. B **812**, 136011 (2021)
30. E. Guzman-Herrera, N. Breton, Light propagation in the vicinity of the ModMax black hole. J. Cosmol. Astropart. Phys. **2024**(01), 041 (2024)
31. B. Heidenreich, M. Reece, T. Rudelius, Evidence for a sublattice weak gravity conjecture. J. High Energy Phys. **2017**(8), 1–40 (2017)

32. B. Heidenreich, M. Reece, T. Rudelius, Sharpening the weak gravity conjecture with dimensional reduction. J. High Energy Phys. **2016**(2), 1–41 (2016)
33. J. Sadeghi et al., RPS thermodynamics of Taub-NUT AdS black holes in the presence of central charge and the weak gravity conjecture. Gen. Relativ. Gravit. **54**(10), 129 (2022)
34. Y. Liu, Higgs inflation and scalar weak gravity conjecture. Eur. Phys. J. C **82**(11), 1052 (2022)
35. Y. Liu, Higgs inflation and its extensions and the further refining dS swampland conjecture. Eur. Phys. J. C **81**(12), 1122 (2021)
36. N. Arkani-Hamed et al., Causality, unitarity, and the weak gravity conjecture. J. High Energy Phys. **2022**(3), 1–36 (2022)
37. B. Heidenreich, M. Reece, T. Rudelius, The weak gravity conjecture and emergence from an ultraviolet cutoff. Eur. Phys. J. C **78**, 1–33 (2018)
38. S. Barbosa, S. Fichet, L. de Souza, On the black hole weak gravity conjecture and extremality in the strong-field regime. arXiv preprint arXiv:2503.20910 (2025)
39. S. Barbosa, P. Brax, S. Fichet, L. de Souza, Running Love numbers and the effective field theory of gravity. arXiv preprint arXiv:2501.18684 (2025)
40. N. Schöneberg et al., News from the Swampland-constraining string theory with astrophysics and cosmology. J. Cosmol. Astropart. Phys. **2023**(10), 039 (2023)
41. S.S. Pal, Weak gravity conjecture, central charges and η/s. arXiv preprint arXiv:1003.0745 (2010)
42. J. Sadeghi, M.R. Alipour, S.N. Gashti, Emerging WGC from the Dirac particle around black holes. Mod. Phys. Lett. A **38**(26–27), 2350122 (2023)
43. S. Kaya, T. Rudelius, Higher-group symmetries and weak gravity conjecture mixing. J. High Energy Phys. **2022**(7), 1–33 (2022)
44. J. Sadeghi et al., de Sitter Swampland conjecture in string field inflation. Eur. Phys. J. C **83**, 635 (2023)
45. N. Craig, I.G. Garcia, S. Koren, Discrete gauge symmetries and the weak gravity conjecture. J. High Energy Phys. **2019**(5), 1–19 (2019)
46. D. Junghans, Large-field inflation with multiple axions and the weak gravity conjecture. J. High Energy Phys. **2016**(2), 1–36 (2016)
47. P. Agarwal, J. Song, Large N gauge theories with a dense spectrum and the weak gravity conjecture. J. High Energy Phys. **2021**(5), 1–11 (2021)
48. S. Brahma, M.W. Hossain, Relating the scalar weak gravity conjecture and the swampland distance conjecture for an accelerating universe. Phys. Rev. D **100**(8), 086017 (2019)
49. J. Yuennan, P. Channuie, Further refining swampland conjecture on inflation in general scalar-tensor theories of gravity. Fortschr. Phys. **70**(6), 2200024 (2022)
50. K. Furuuchi, Weak gravity conjecture from low energy observers' perspective. Fortschr. Phys. **66**(10), 1800016 (2018)
51. J. Sadeghi et al., Can black holes cause cosmic expansion?. arXiv preprint arXiv:2305.12545 (2023)
52. D. Lüst, P. Eran, Scalar fields, hierarchical UV/IR mixing and the weak gravity conjecture. J. High Energy Phys. **2018**(2) (2018)
53. J. Sadeghi, M.R. Alipour, S.N. Gashti, Scalar weak gravity conjecture in super Yang–Mills inflationary model. Universe **8**(12), 621 (2022)
54. J. Sadeghi et al., Weak gravity conjecture from conformal field theory: a challenge from hyperscaling violating and Kerr–Newman-AdS black holes. Chin. Phys. C **47**(1), 015103 (2023)
55. R. Solomon, D. Stojkovic, Generalizing weak gravity conjecture. Phys. Rev. D **102**(4), 046016 (2020)
56. M. Montero, A holographic derivation of the weak gravity conjecture. J. High Energy Phys. **2019**(3), 1–44 (2019)
57. K. Nakayama, F. Takahashi, T.T. Yanagida, Revisiting the number-theory dark matter scenario and the weak gravity conjecture. Phys. Lett. B **790**, 218–224 (2019)
58. W.H. Kinney, S. Vagnozzi, L. Visinelli, The zoo plot meets the swampland: mutual (in) consistency of single-field inflation, string conjectures, and cosmological data. Class. Quantum Gravity **36**(11), 117001 (2019)
59. J. Sadeghi, S. Noori Gashti, E. Naghd Mezerji, The investigation of universal relation between corrections to entropy and extremality bounds with verification WGC. Phys. Dark Universe **30**, 100626 (2020)
60. P. Agrawal et al., On the cosmological implications of the string swampland. Phys. Lett. B **784**, 271–276 (2018)
61. S.D. Odintsov, V.K. Oikonomou, Swampland implications of GW170817-compatible Einstein–Gauss–Bonnet gravity. Phys. Lett. B **805**, 135437 (2020)
62. J. Sadeghi et al., Strong cosmic censorship in light of weak gravity conjecture for charged black holes. J. High Energy Phys. **2023**(2), 1–14 (2023)
63. J. Yuennan, P. Channuie, Composite Inflation and further refining dS swampland conjecture. Nucl. Phys. B **986**, 116033 (2023)
64. J. Sadeghi et al., Weak gravity conjecture, black branes and violations of universal thermodynamics relation. Ann. Phys. **447**, 169168 (2022)
65. J. Yuennan, P. Channuie, Further refining swampland conjecture on inflation in general Scalar-Tensor theories of gravity. Fortschr. Phys. **70**(6), 2200024 (2022)
66. J. Sadeghi, B. Pourhassan, S. Noori Gashti, S. Upadhyay, Swampland conjecture and inflation model from brane perspective. Phys. Scr. **96**, 125317 (2021)
67. S. Noori Gashti, J. Sadeghi, B. Pourhassan, Pleasant behavior of swampland conjectures in the face of specific inflationary models. Astropart. Phys. **139**, 102703 (2022)
68. J. Sadeghi, B. Pourhassan, S. Noori Gashti, E. Naghd Mezerji, A. Pasqua, Cosmic evolution of the logarithmic f(R) model and the dS swampland conjecture. Universe **8**(12), 623 (2022)
69. J. Sadeghi, B. Pourhassan, S. Noori Gashti, I. Sakalli, M.R. Alipour, de Sitter swampland conjecture in string field inflation. Eur. Phys. J. C **83**, 635 (2023)
70. S.N. Gashti, Two-field inflationary model and swampland de Sitter conjecture. J. Hologr. Appl. Phys. **2**(1), 13–24 (2022). https://doi.org/10.22128/jhap.2021.452.1002
71. Y. Abe, T. Noumi, K. Yoshimura, Black hole extremality in nonlinear electrodynamics: a lesson for weak gravity and Festina Lente bounds. J. High Energy Phys. **2023**(9), 1–38 (2023)
72. P. Bittar, S. Fichet, L. de Souza, Gravity-induced photon interactions and infrared consistency in any dimensions. arXiv preprint arXiv:2404.07254 (2024)
73. S.N. Gashti et al., Noncommutativity and its role in constant-roll inflation models with non-minimal coupling constrained by swampland conjectures. Chin. Phys. C **49**(2), 025108 (2025)
74. P. Lin, A. Mininno, G. Shiu, Formulating the weak gravity conjecture in AdS space. arXiv preprint arXiv:2503.05862 (2025)
75. J. Sadeghi et al., Swampland conjectures and noncommutative phase space in the constant-roll inflation with Brans–Dicke cosmology. Int. J. Theor. Phys. **63**(12), 1–20 (2024)
76. M. Etheredge, B. Heidenreich, N. Pittman, S. Rauch, M. Reece, T. Rudelius, Confined monopoles and failure of the lattice weak gravity conjecture. arXiv preprint arXiv:2502.14951 (2025)
77. A. Anand, S.N. Gashti, Universal relations with the non-extensive entropy perspective. arXiv preprint arXiv:2411.02875 (2024)
78. T. Antonelli, X. Calmet, The weak gravity conjecture in the Vilkovisky–DeWitt effective action of quantum gravity. Phys. Lett. B **18**, 139403 (2025)
79. S.N. Gashti, M.R. Alipour, M.A.S. Afshar, Exploring the parameter space of inflation model on the brane and its compatibility with

the swampland conjectures. arXiv preprint arXiv:2409.06488 (2024)
80. Y. Xiao, Q. Wang, A. Zhang, A proof of the weak gravity conjecture via leading-order quantum gravity effects. arXiv preprint arXiv:2503.08459 (2025)
81. M.P. Hertzberg, R. Nathan, S.E. Semaan, Solar system constraints on light propagation from higher derivative corrections to general relativity and the weak gravity conjecture. arXiv preprint arXiv:2503.19236 (2025)
82. A. Tokareva, Y. Xu, Scalar weak gravity bound from full unitarity. arXiv preprint arXiv:2502.10375 (2025)
83. A. Anand, Thermodynamic extremality in Power-law AdS black holes: a universal perspective. Eur. Phys. J. C **85**(3), 1–13 (2025)
84. A. Anand, A. Mishra, P. Channuie, Stability of extremal black holes and weak cosmic censorship conjecture in Kiselev spacetime. arXiv preprint arXiv:2411.02427 (2024)
85. B.E. Panah, Analytic electrically charged black holes in F (R)-ModMax theory. Prog. Theor. Exp. Phys. **2024**(2), 023E01 (2024)
86. A. de La Cruz-Dombriz, A.A.L.M. Dobado, A.L. Maroto, Black holes in f (R) theories. Phys. Rev. D Part. Fields Gravit. Cosmol. **80**(12), 124011 (2009)
87. T. Moon, Y.S. Myung, E.J. Son, f (R) black holes. General Relativ. Gravit. **43**, 3079–3098 (2011)
88. S.-W. Wei, Y.-X. Liu, R.B. Mann, Black hole solutions as topological thermodynamic defects. Phys. Rev. Lett. **129**(19), 191101 (2022)
89. S.-W. Wei, Y.-X. Liu, Topology of black hole thermodynamics. Phys. Rev. D **105**(10), 104003 (2022)
90. N.-C. Bai, L. Li, J. Tao, Topology of black hole thermodynamics in Lovelock gravity. Phys. Rev. D **107**(6), 064015 (2023)
91. P.K. Yerra, C. Bhamidipati, Topology of Born–Infeld AdS black holes in 4D novel Einstein–Gauss–Bonnet gravity. Phys. Lett. B **835**, 137591 (2022)
92. J. Sadeghi et al., Bardeen black hole thermodynamics from topological perspective. Ann. Phys. **455**, 169391 (2023)
93. D. Wu, Topological classes of thermodynamics of the four-dimensional static accelerating black holes. Phys. Rev. D **108**(8), 084041 (2023)
94. D. Wu, W. Shuang-Qing, Topological classes of thermodynamics of rotating AdS black holes. Phys. Rev. D **107**(8), 084002 (2023)
95. J. Sadeghi et al., Bulk-boundary and RPS thermodynamics from topology perspective. Chin. Phys. C (2024)
96. D. Wu et al., Topological classes of thermodynamics of the static multi-charge AdS black holes in gauged supergravities. arXiv preprint arXiv:2402.00106 (2024)
97. Y. Sekhmani et al., Thermodynamic topology of black holes in $F(R)$-Euler–Heisenberg gravity's rainbow. arXiv preprint arXiv:2409.04997 (2024)
98. N.J. Gogoi, P. Phukon, Thermodynamic topology of 4D dyonic AdS black holes in different ensembles. Phys. Rev. D **108**(6), 066016 (2023)
99. B. Hazarika, P. Phukon, Thermodynamic topology of D = 4, 5 Horava Lifshitz black hole in two ensembles. Nucl. Phys. B **1006**, 116649 (2024)
100. J. Sadeghi et al., Topology of Hayward-AdS black hole thermodynamics. Phys. Scr. **99**(2), 025003 (2024)
101. J. Sadeghi et al., Thermodynamic topology and photon spheres in the hyperscaling violating black holes. Astropart. Phys. **156**, 102920 (2024)
102. B. Hazarika, P. Prabwal, Thermodynamic topology of black holes in f (R) gravity. Prog. Theor. Exp. Phys. **2024**(4), 043E01 (2024)
103. D. Wu, Topological classes of thermodynamics of the four-dimensional Lorentzian charged Taub-NUT spacetimes. Eur. Phys. J. C **83**(7), 589 (2023)
104. B. Hazarika, B. Eslam Panah, P. Phukon, Thermodynamic topology of topological charged dilatonic black holes. arXiv preprint arXiv:2407.05325 (2024)
105. S.N. Gashti, S. Izzet, P. Behnam, Thermodynamic topology, photon spheres, and evidence for weak gravity conjecture in charged black holes with perfect fluid within Rastall theory. arXiv preprint arXiv:2410.14492 (2024)
106. M.A.S. Afshar, S. Jafar, Mutual influence of photon sphere and non-commutative parameter in various non-commutative black holes: part I-towards evidence for WGC. arXiv preprint arXiv:2411.09557 (2024)
107. B. Eslam Panah, B. Hazarika, P. Phukon, Thermodynamic topology of topological black hole in F (R)-ModMax gravity's rainbow. Prog. Theor. Exp. Phys. **2024**(8), 083E02 (2024)
108. D. Wu, Consistent thermodynamics and topological classes for the four-dimensional Lorentzian neutral NUT-charged spacetimes. Eur. Phys. J. C **83**(5), 365 (2023)
109. D. Wu, Classifying topology of consistent thermodynamics of the four-dimensional neutral NUT-charged spacetimes. Eur. Phys. J. C **83**(5), 365 (2023)
110. S.-P. Wu, S.-W. Wei, Thermodynamical topology of quantum BTZ black hole. Phys. Rev. D **110**(2), 024054 (2024)
111. J. Sadeghi et al., Bulk-boundary and RPS thermodynamics from topology perspective. Chin. Phys. C (2024)
112. J. Sadeghi et al., Thermodynamic topology of quantum corrected AdS-Reissner–Nordstrom black holes in Kiselev spacetime. Chin. Phys. C (2024)
113. H. Bidyut, P. Phukon, Thermodynamic properties and shadows of black holes in f(R,T) gravity. arXiv:2410.00606v1 (2024)
114. R. Hemant, R. Dibakar, Topology of black hole phase transition in JT gravity. arXiv:2410.00744 (2024)
115. S.N. Gashti et al., Thermodynamic topology of Kiselev-AdS black holes within f (R, T) gravity. Chin. Phys. C **49**(3), 035110 (2025)
116. A.B. Brzo et al., Thermodynamic topology of AdS black holes within non-commutative geometry and barrow entropy. Nucl. Phys. B **1012**, 116840 (2025)
117. S.N. Gashti et al., Thermodynamic topology and photon spheres of dirty black holes within non-extensive entropy. Phys. Dark Universe **47**, 101833 (2025)
118. M.A.S. Afshar et al., Topological insights into black hole thermodynamics: non-extensive entropy in CFT framework. arXiv preprint arXiv:2501.00955 (2025)
119. S.N. Gashti, B. Pourhassan, I. Sakallı, Thermodynamic topology and phase space analysis of AdS black holes through non-extensive entropy perspectives. Eur. Phys. J. C **85**(3), 305 (2025)
120. S.N. Gashti, Topology of holographic thermodynamics within non-extensive entropy. J. Hologr. Appl. Phys. **4**(4), 59–70 (2024). arXiv:2412.00889
121. M.R. Alipour et al., Topological classification and black hole thermodynamics. Phys. Dark Universe **42**, 101361 (2023)